

SWEET-Cat updated ★ ★★

New homogenous spectroscopic parameters

S. G. Sousa¹, V. Adibekyan¹, E. Delgado-Mena¹, N. C. Santos^{1,2}, D. T. Andreasen¹, A. C. S. Ferreira¹, M. Tsantaki¹, S. C. C. Barros¹, O. Demangeon¹, G. Israelian³, J. P. Faria¹, P. Figueira^{4,1}, A. Mortier⁵, I. Brandão¹, M. Montalto⁶, B. Rojas-Ayala⁷, and A. Santerne^{8,1}

¹ Instituto de Astrofísica e Ciências do Espaço, Universidade do Porto, CAUP, Rua das Estrelas, 4150-762 Porto, Portugal

² Departamento de Física e Astronomia, Faculdade de Ciências, Universidade do Porto, Rua do Campo Alegre, 4169-007 Porto, Portugal

³ Instituto de Astrofísica de Canarias, 38200 La Laguna, Tenerife, Spain

⁴ European Southern Observatory, Alonso de Cordova 3107, Vitacura, Santiago, Chile

⁵ Centre for Exoplanet Science, SUPA, School of Physics and Astronomy, University of St Andrews, St Andrews KY16 9SS, UK

⁶ Dipartimento di Fisica e Astronomia "Galileo Galilei", Università di Padova, Vicolo dell'Osservatorio 3, Padova IT-35122, Italy

⁷ Departamento de Ciencias Físicas, Universidad Andres Bello, Fernandez Concha 700, Las Condes, Santiago, Chile

⁸ Aix Marseille Univ, CNRS, CNES, LAM, Marseille, France

Received September 15, 1996; accepted March 16, 1997

ABSTRACT

Context. Exoplanets have now been proven to be very common. The number of its detections continues to grow following the development of better instruments and missions. One key step for the understanding of these worlds is their characterization, which mostly depend on their host stars.

Aims. We perform a significant update of the Stars With ExoplanETs CATalog (SWEET-Cat), a unique compilation of precise stellar parameters for planet-host stars provided for the exoplanet community.

Methods. We made use of high-resolution spectra for planet-host stars, either observed by our team or found in several public archives. The new spectroscopic parameters were derived for the spectra following the same homogeneous process (ARES+MOOG). The host star parameters were then merged together with the planet properties listed in exoplanet.eu to perform simple data analysis.

Results. We present new spectroscopic homogeneous parameters for 106 planet-host stars. Sixty-three planet hosts are also reviewed with new parameters. We also show that there is a good agreement between stellar parameters derived for the same star but using spectra obtained from different spectrographs. The planet-metallicity correlation is reviewed showing that the metallicity distribution of stars hosting low-mass planets (below 30 M_{\oplus}) is indistinguishable from that from the solar neighborhood sample in terms of metallicity distribution.

Key words. Planets and satellites: formation Planets and satellites: fundamental parameters Stars: abundances Stars: fundamental parameters

1. Introduction

The first extrasolar planets around solar-type stars to be discovered, hot jupiters, have completely changed our understanding of planet formation and evolution based on the solar system alone (e.g., Mayor & Queloz 1995). The surprises were far from over and in recent years, with the detection of smaller and lower mass planets, and our theoretical view continues to be shaped by the observational evidence. Today ~ 3800 extrasolar planets have been discovered orbiting ~ 2800 solar-type stars (exoplanet.eu Schneider et al. 2011). The higher numbers of discoveries al-

lows us to perform better statistical studies on the different types of planetary systems.

Although today we are convinced that extrasolar planets are present around almost every (dwarf or main sequence) star (e.g., Mayor et al. 2011), the first observational evidence, based on the first massive planets detections, showed that planets were more frequently orbiting metal-rich stars (e.g., Santos et al. 2004; Valenti & Fischer 2005). Soon after, it was reported that the metallicity correlation was not clear for the first detections of lower mass and small planets (e.g., Sousa et al. 2008; Ghezzi et al. 2010; Schlaufman & Laughlin 2011; Buchhave et al. 2012; Wang & Fischer 2015; Buchhave & Latham 2015). Other observational evidence has been reported involving the host stellar properties and the properties of planets. Correlations such as the planetary radius versus metallicity (e.g., Buchhave et al. 2014; Schlaufman 2015), planet-period versus metallicity, or eccentricity versus metallicity (e.g., Beaugé & Nesvorný 2013; Adibekyan et al. 2013; Dawson et al. 2015; Mulders et al. 2016; Wilson et al. 2018), all show interesting evidence that is important for the understanding of planet formation. It is therefore cru-

* Based on observations collected at the European Organisation for Astronomical Research in the Southern Hemisphere under ESO programs 096.C-0092, 097.C-0280, 098.C-0151, and data obtained from the ESO Science Archive Facility under several requests (request numbers 273579-274977).

** Tables A.1-A.3 are also available in electronic form at the CDS via anonymous ftp to cdsarc.u-strasbg.fr (130.79.128.5) or via <http://cdsweb.u-strasbg.fr/cgi-bin/qcat?J/A+A/>

cial not only to increase the number of discoveries but also to characterize planetary systems precisely since they play a fundamental role in the interpretation of these results.

Precise and accurate fundamental planetary parameters (mass, radius, and mean density) are needed to distinguish between solid rocky, water rich, or otherwise gas dominated planets. To achieve this we need a precision of planetary mass up to 10% and a radius up to 5% (or even 2% for further bulk characterization; e.g., Wagner et al. 2011; Bean et al. 2011). The derivation and precision of the planetary properties depends considerably on the deduced parameters of the stellar host (e.g., Bouchy et al. 2004; Torres et al. 2012; Mortier et al. 2013b; Sousa et al. 2015b). Interestingly, it has been shown that the quality of the spectroscopic and photometric observations affects the properties of the planets more significantly than the model-dependent systematics, such as using different stellar evolution models for the determination of stellar mass and radius (e.g., Southworth 2009). It is therefore extremely important to use high-quality data to refine the values for these stellar properties in order to obtain more precise and accurate stellar masses and radii and thus more precise and accurate planetary masses and radii. Furthermore, to minimize global statistical errors, a uniform analysis is required (see, e.g., Torres et al. 2012) to guarantee homogeneity of the results. Using different methods to derive stellar properties leads to discrepancies in the results which, in turn, deteriorates the significance of the statistical analyses.

For this reason a great effort has been made in the creation and continuous update of the currently largest homogeneous catalog of stellar parameters for planet hosts (SWEET-Cat¹) first presented in Santos et al. (2013), and then updated with new parameters for a significant number of planet hosts in Sousa et al. (2015b) and in Andreasen et al. (2017). In this work we continue the series of SWEET-Cat papers using our uniform method, which has been tested and improved upon extensively. We collected spectra from different spectrographs to derive new homogeneous stellar parameters for 106 planet hosts. We then use the updated catalog to review the metallicity correlations and make these parameters available for the community; these new values can be used for further statistical studies in the quest for clues for the formation and evolution of the planets.

The work is divided into the following sections: Section 2 describes the spectroscopic data compilation for SWEET-Cat, together with some details on spectra characteristics that our team has compiled to date. Section 3 shows results for the new spectroscopic stellar parameters derived as well as a comparison with literature values. In addition we show that the homogenization of our method is valid with the use of many different high-resolution spectrographs. Section 4 presents some up-to-date metallicity correlations relevant for planet formation. We conclude in Section 5 with a summary of the work presented.

2. Spectroscopic data

In this section we describe the spectroscopic data used to derive stellar parameters in recent years. Some of this data were already relatively old (more than ten years), obtained from different spectrographs, and were already used in previous works. These were collected from observations with diverse scientific goals, mostly from radial-velocity (RV) planet surveys (e.g., HARPS), and other data were obtained specifically for planet-host spectroscopic stellar characterization (e.g., FEROS and UVES). To better describe all sources of the different spectroscopic data used

today for SWEET-Cat, we divided the discussion into the following items: legacy data, recent observations, and public data from spectroscopic archives.

2.1. Compiling legacy spectroscopic data

One of the goals of this work was to compile all the spectra that our team has used in the past works which provides parameters for SWEET-Cat. The list of spectrographs used in SWEET-Cat is already relatively large and can be seen in Table 1. We compiled all the spectra from our previous works in the literature to derive the stellar parameters. These include Ammler-von Eiff et al. (2009); Andreasen et al. (2017); Boisse et al. (2010, 2012); Bonomo et al. (2012); Damasso et al. (2015); Delgado Mena et al. (2014); Díaz et al. (2012, 2016); Gillon et al. (2007); Gómez Maqueo Chew et al. (2013); Hébrard et al. (2010, 2016); Lillo-Box et al. (2016); Melo et al. (2007); Montalto et al. (2012); Mortier et al. (2013a,b); Moutou et al. (2006, 2011, 2014, 2015); Neves et al. (2013, 2014); Osborn et al. (2017); Pont et al. (2008); Rey et al. (2017); Sahlmann et al. (2011); Santerne et al. (2014, 2016); Santos et al. (2004, 2005, 2006, 2008, 2013); Ségransan et al. (2010); Sousa et al. (2006, 2008, 2011a,b, 2015b); Tamuz et al. (2008); Tsantaki et al. (2013, 2014); Udalski et al. (2008); Wilson et al. (2016); da Silva et al. (2007).

The original data formats depend on several factors such as the instrument used or the pipeline used to process the data. Most of the spectra are stored in standard Flexible Image Transport System (FITS) files, but some were stored in text format. In order to homogenize all the data we made sure that all the individual spectra were stored in a standard 1D fit format, easy to read by standard routines and in particular by the Automatic Routine for line Equivalent widths in stellar Spectra (ARES; see Sousa et al. 2007, 2015a), which requires specific FITS header keywords (e.g., CDEL1 and CRVAL1).

It is not our goal here to completely describe all the details of this technical step, but rather to provide a short description. Most of the spectra were already reduced and stored in this format. For the text files, the transformation is trivial, unless the wavelength spacing is not constant. In these cases we interpolated the spectra to derive an evenly spaced wavelength coverage, which is a requirement for the adopted FITS format. The 2D echelle reduced spectra actually needed more caution for the correct transformation into the standard 1D spectra. For the blaze-corrected and normalized 2D spectrum, the transformation is trivial and a simple merging of the orders was performed; we took special caution when the orders overlapped in wavelength. For these we used the *scombine* routine in Image Reduction and Analysis Facility (IRAF) that allow us to combine different orders into a 1D spectrum. For rather old spectra (e.g., SARG and some old FIES observations) the 2D spectra are still contaminated with the blaze function. To make the situation more complex, in a few cases there were also some strange peak structures in the limits of the orders, most likely due to reduction problems. These creates difficulties for an automatic merging of the orders and for those cases we went spectra by spectra, order by order, to clean out the peak structures in the spectra as best as possible before the merging of the orders into a 1D spectrum.

2.2. Recent spectroscopic observations and data reduction

During recent years several of our ESO proposals have been successfully awarded with which we obtained high-resolution spec-

¹ www.astro.up.pt/resources/sweet-cat

Table 1. Spectrographs used in SWEET-Cat

Spectrograph	Spec range (Å)	R	Observatory
HARPS	3600 - 6900	110000	ESO La Silla (Chile)
UVES	4800 - 6800	100000	ESO Paranal (Chile)
CORALIE	3900 - 6800	50000	ESO La Silla (Chile)
ESPADONS	3700 - 10500	80000	CHFT (USA)
FEROS	3800 - 9200	48000	ESO La Silla (Chile)
SOPHIE	3872 - 6943	75000	OHP (France)
ELODIE	3895 - 6815	42000	OHP (France)
SARG	3700 - 10000	85000	ORM (Spain)
NARVAL	3700 - 10500	80000	TBL (France)
FIES	3700 - 8300	67000	ORM (Spain)
UES	3600 - 7250	55000	ORM (Spain)

Notes. Many of these spectrographs have different configurations available for observation. We list the typical spectral range and resolution for the observations that we collected or found in archives.

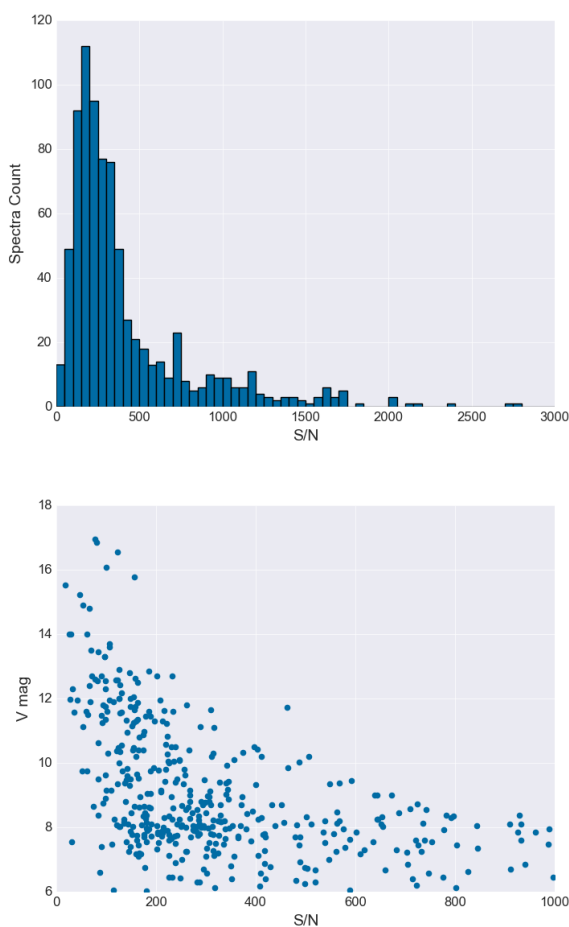


Fig. 1. S/N distribution (top panel) and S/N vs. V magnitude (bottom panel) for SWEET-Cat spectral data. The bottom panel is cut at S/N of 1000 for a better visualization of the correlation.

tra with UVES (Dekker et al. 2000) at the UT2 telescope in Paranal, Chile. The spectra that we have collected in recent ESO periods include programs 096.C-0092, 097.C-0280, and 098.C-0151.

In all these proposals we took advantage of the use of Image Slicer #3, which allows us to observe with poor seeing conditions and still catches most of the flux. Since we used a line

Table 2. Statistics of SWEET-Cat as of April 2018

Number	Description
2631	stars in SWEET-Cat (linked from exo.eu)
808	individual stellar spectra (different instruments)
653	stars with spectra
562	planet hosts with homogeneous parameters
541	FGK stars with homogeneous parameters
113	stars with spectra but no homogeneous parameters
106	new parameters included in this work
123	stars without spectra with $V < 12$

by line analysis in our procedures, we proposed to observe with the smallest slit (0.3"), which gives a higher resolution for a better spectroscopic analysis. The typical spectra configuration used for UVES is RED580, which covers the optical spectrum in the interval 476-684nm; this allows us to observe many lines of different elements. The spectra collected in these proposals are supposed to achieve a S/N of 300 for the stars brighter than $V=10$ and S/N of 150 for the faintest stars. For the brightest stars single exposures are enough to reach the requested S/N. For the fainter stars we choose to divide the requested exposure times in chunks of a maximum of 1800 seconds of exposure. With this observational strategy, we avoid the overpopulation of cosmic rays, which becomes more difficult to correct for large exposure times.

The data reduction of these observations were carried out using the UVES Pipeline in Reflex (Freudling et al. 2013) provided by ESO following the standard recipes and suggestions mentioned in the UVES pipeline manual to reduce UVES data observed with the image slicer.

The combination of the spectra was then carried out using the IRAF routine *scombine*, which was used to combine the RED1 and REDu spectra observations, and later this routine was used to combine these spectra into one final 1D spectrum.

2.3. Spectra from the public archives

Most of the public data that we were able to find came from the ESO archive² with the help of *astroquery*³; more specifically we looked for reduced data, which are also available. We looked for relatively high resolution and good S/N (also considering possible combinations of low S/N individual spectra). We selected the ESO instruments FEROS, HARPS, and UVES for this search in this archive. When many spectra were available for the same star, probably coming from RV planet search surveys, we downloaded a sufficient number of spectra to reach a S/N of about 2000. We note that these S/N values comes directly from photon counts and the real S/N should depend on other noise sources (e.g., background subtraction). Also, for the faint stars in the archive, when sufficient spectra were available, we discarded the very low S/N spectra for the combination. To give an idea of the amount of data collected from ESO during this process we made more than 100 archive requests with around 34 Gb of data in total. Other archives were also used to search for spectra for

² http://archive.eso.org/eso/eso_archive_main.html

³ <http://astroquery.readthedocs.io>

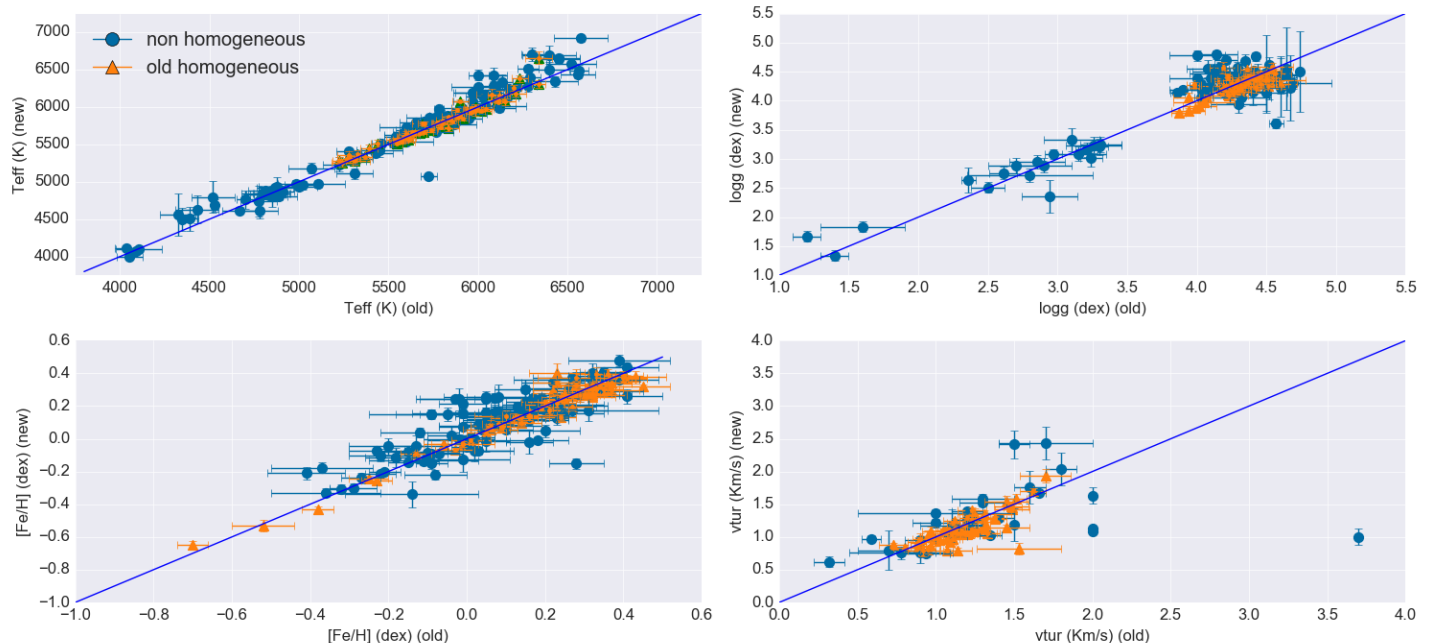


Fig. 2. Comparison between old parameters listed in SWEET-Cat and the new parameters derived in this work. The blue filled circles represent parameters with recent spectroscopic data. The orange triangles represent new rederived parameters with legacy spectroscopic data.

SWEET-Cat. These include current public archives containing spectra from SOPHIE⁴, ESPADONS⁵, and FIES⁶.

2.4. SWEET-Cat spectroscopic data statistics

As of April 2018 we had a total of 2 631 planet-host stars (source exoplanet.eu). We were able to gather spectra for 653 of these, including the new sources presented in this work. The reason for this relatively low number of stars with spectra is because many are relatively faint stars observed by Kepler (Borucki et al. 2010). Given the faintness of the majority of these stars, it is clear that the observation and the collection of high-quality, high-resolution spectra is quite difficult and costly. On top of that, Kepler stars are not observable from ESO facilities, which are our most direct source of data. When considering bright stars, which is also fundamental for RV follow up and planetary mass measurements (Fortier et al. 2014; Rauer et al. 2014), the percentage of stars with spectra and homogeneous parameters becomes quite high. With the work presented in this paper, considering the addition of 106 new stars with homogeneous parameters, we have $\sim 90\%$ and $\sim 80\%$ completeness for stars with $V < 9$ and $V < 12$, respectively. Completeness represents the number of planet hosts with homogeneous spectroscopic parameters relative to the number of stars with planets in SWEET-Cat.

Table 2 sums up some numbers relative to the planet hosts and their spectra collected using different instruments as well as the number of stars with derived homogeneous parameters. We note that we have seven planet-hosts stars with low-quality spectra in the database for which we did not derive reliable parameters. A histogram of the S/N for all the final combined SWEET-Cat spectra is also presented in the top panel of Fig. 1. The S/N value was derived automatically using the same procedure as used in the ARES code and considering the recommended spec-

tral regions (Sousa et al. 2015a). Most of the very high S/N spectra come from the combination of several spectra observed during RV programs. The correlation between the S/N of our spectra with the V magnitude of the planet-host stars is also clear (see bottom panel of Fig. 1).

3. Stellar parameters

3.1. Spectroscopic parameters and stellar masses

The spectroscopic analysis was carried out with "ARES+MOOG" (In this work we used ARES v2, and MOOG2014. For more details, see Sousa 2014) both for the new spectroscopic data and for part of the legacy data that already had derived homogeneous parameters before 2008. The analysis is based on the excitation and ionization balance of iron abundance, where the absorption lines are consistently measured with the ARES code (Sousa et al. 2007, 2015a) and the abundances are derived in local thermodynamic equilibrium (LTE) with the MOOG code (Sneden 1973) and uses a grid of Kurucz ATLAS9 plane-parallel model atmospheres (Kurucz 1993). The same methodology can also be applied with FASMA⁷ (Andreasen et al. 2017). The method has been applied in our previous spectroscopic studies of planet hosts (e.g., Sousa et al. 2008, 2011a; Mortier et al. 2013b; Sousa et al. 2015b).

The line list used here was that from Sousa et al. (2008) except for the stars whose effective temperature is below 5200 K ($T_{eff} < 5200K$). For these stars we rederived parameters using a more adequate line list for cooler stars, which was compiled by Tsantaki et al. (2013). The atomic data, log gfs, were recalibrated in the same way as in previous works, but in this work we used MOOG2014. There are small changes in log gf values, which most likely come from numerical differences from a different compilation of the code.

The stellar masses presented in this work were derived with the calibration presented in Torres et al. (2010) and a correction

⁷ <http://www.iastro.pt/fasma/>

⁴ <http://atlas.obs-hp.fr/sophie/>

⁵ <http://www.cadc-ccda.hia-ihp.nrc-cnrc.gc.ca/en/cfht/>

⁶ <http://www.not.iac.es/archive/>

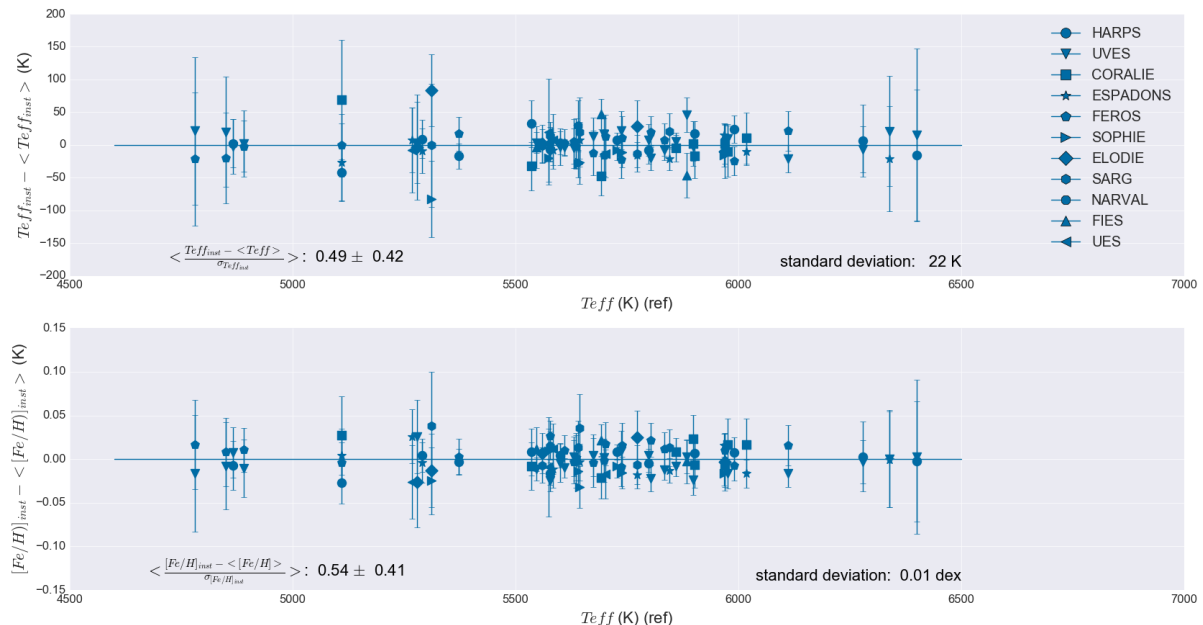


Fig. 3. Comparison between parameters derived from different spectrographs with ARES+MOOG.

presented in Santos et al. (2013) was applied for the cases in which the calibration gives values between 0.7 and 1.3 M_{\odot} . The errors for these mass values are computed as in Santos et al. (2013), where for each case 10 000 random values of effective temperature, surface gravity, and stellar metallicity were drawn from a Gaussian distribution. We used the uncertainties of the spectroscopic parameters this way to estimate the distribution of the derived mass. The error for the mass is extracted from the standard deviation of this mass distribution for each star.

Table 4 presents the new parameters derived with ARES+MOOG in this work for the new spectra collected. In this table we report the spectroscopic parameters (effective temperature (T_{eff}), surface gravity ($\log g_{\text{spec}}$), microturbulence (ξ), and iron abundance ($[\text{Fe}/\text{H}]$ - used as a proxy for metallicity), the number of iron lines used in the spectroscopic analysis, and the stellar mass. This table also presents the instrument and a column identifying which parameters are adopted for the planet hosts in the SWEET-Cat online table.

We note that in Sousa et al. (2008) we also used High-Precision PARallax Collecting Satellite (HIPPARCOS) parallaxes to derive surface gravities, and in that work we observed some differences between the spectroscopic and trigonometric $\log g$. However, although the spectroscopic surface gravity is the less constrained parameter in our analysis, the positive side is that the other parameters (T_{eff} and $[\text{Fe}/\text{H}]$) are almost independent of the $\log g$. This means that when fixing the $\log g$ to a different value derived with the use of parallaxes, interferometry, and asteroseismology we do not see any significant changes in the other parameters. In the online table the $\log g$ values listed are those directly derived from our spectroscopic analysis and are not corrected for known systematics, but we suggest the user employ the corrections discussed in Mortier et al. (2014).

There are also a few stars for which the application of an equivalent width, such as the ARES+MOOG method, is not appropriate owing to strong blends in the spectra. Some of these stars reveal a relatively high stellar rotation ($\gtrsim 10$ -15 Km/s) and

others are quite cool stars ($T_{\text{eff}} \lesssim 4200$ K). For these stars we applied a method based on synthetic spectra, which preserves the homogeneity; this method is described in Tsantaki et al. (2014), in which we have shown that the parameters derived in this way are in the same scale as the parameters derived by our Equivalent Width (EW) method. The parameters for these 11 stars are presented in Table 5. For these stars we were also able to derive the rotational velocity ($v \sin(i)$).

In SWEET-Cat there are a significant amount of planet hosts, for which the spectroscopic parameters were derived more than ten years ago. These represent some of the first planets discovered, many of which are hot jupiters for which the spectroscopic analysis was based on a smaller line list of iron lines (e.g., Santos et al. 2004). We have shown that these parameters are consistent and in the same scale as those derived with the current largest line lists (Sousa et al. 2008; Tsantaki et al. 2013). Consequently, we took the opportunity to run our codes with these line lists for the whole sample to reanalyze these stars with the current method, which gives more statistical strength to the results. Therefore, all the spectroscopic parameters that were derived with this small line list were rederived in this work. Table 6 presents the results for these planet-host stars.

Figure 2 shows the comparison between the new spectroscopic parameters derived in this work against the previous (in the literature) parameters reported in SWEET-Cat mostly coming from planet discovery papers. The blue circles represent new planet hosts for which, for the first time, we use our method to derive parameters. The orange triangles represent the planet hosts for which we had already reported homogeneous parameters but using the small line list. As we already mentioned before we show a very good consistency between the new and previous homogeneous parameters. The gain is mainly related to the use of more lines, which statistically are translated into smaller precision errors. For the completely new homogeneous data (blue circles; 106 planet hosts) we have a general good consistency with the literature data where the largest differences appear for

evolved stars (lower surface gravities). The lower number of points for the microturbulence comes from the fact that many of the spectroscopic analyses available from the literature for these stars do not report this parameter.

3.2. Different Instruments

One of the main advantages of SWEET-Cat is the homogenization of the spectroscopic parameters derived by our team. A possible problem that could affect the homogenization would be the use of different instruments. Actually the use of the same instrument, with the same configuration, is normally considered a very good argument to maintain the homogenization of the spectroscopic analysis. Moreover, there are works such as Bedell et al. (2014) stating that the largest effect is associated with the use of different instruments, which can go up to 0.04 dex in metallicity. Recently we had also shown that even using the same instrument, but with different individual observations of the same star at different times and conditions, can reveal some non-negligible differences in derived individual abundances (Adibekyan et al. 2016). Therefore, it is fundamental to understand how good the homogeneity is in SWEET-Cat when using different instruments.

To answer this relevant question we can make use of our already large compilation of spectroscopic data to test our method against the use of different instruments/configurations. Figure 3 shows the differences found using ARES+MOOG on spectra of the same stars observed with different instruments. In this plot we merge different instruments and, although most of the comparisons are made with only two spectrographs, there is a wide variety of different pairings to access any possible biases with different instruments. Also there are a few stars that were observed by up to four to five different spectrographs. Looking at this figure and comparing the effective temperatures and [Fe/H] it is clear that the values derived are quite consistent when using different instruments. The standard deviation of the parameters relative to the averaged value, used as a reference for each star, is quite small at 22 K for temperature and 0.01 dex for [Fe/H]. It is true that there are some large individual differences for temperatures that can be as high as 100 K in some cases, but they are actually well within the errors reported for those cases. Moreover, the average relative discrepancy from the average is consistent with or below one for all the instruments ($\langle \frac{T_{eff_{inst}} - \langle T_{eff} \rangle}{\sigma_{T_{eff_{inst}}}} \rangle \lesssim 1$). This simple test demonstrates that our spectroscopic method is quite insensitive to the source of the spectroscopic data. It is worth mentioning that most of the spectroscopic data compiled is generally of very good quality, both in terms of S/N and resolution (see Figure 1 and Table 1).

In what regards the selection of the parameters to be listed in SWEET-Cat for the stars for which we have multiple instruments, we selected the values with the lowest estimated errors. We selected this instead of the average because there are cases in which the average can still be significantly affected by the presence of lower quality spectra from other instruments. This is of course strongly correlated with the number of lines used in each analysis and the individual precision of each line and therefore the spectroscopic data with higher resolution and higher S/N spectra are usually selected.

4. Planet-host metallicity correlations

One of the first observational constraints for planet formation theories was the correlation between the presence of giant planets and the higher metallicity of their host stars (e.g., Santos et al.

2004; Fischer & Valenti 2005). Of course, because of the known observational biases from the main planet detection methods, the first planets found were giants and massive. Very soon the correlation was tested for lower mass planets, where, despite the low statistic significance of the first results, the correlation was not observed (e.g., Udry et al. 2006; Sousa et al. 2008; Ghezzi et al. 2010; Sousa et al. 2011a; Buchhave et al. 2012). More recently, Wang & Fischer (2015) suggested that there should be an universal planet-metallicity correlation for all planets, but this might be related to the higher planet frequency and lower detectability of low-mass planets (LMPs; see also Zhu et al. 2016). Once settled, these observational correlations, should provide strong constraints for the theory of planet formation and evolution. In this section we take advantage of our largest sample of planet-host stars with uniform parameters to review the metallicity correlation.

Figure 4 shows the metallicity distribution of planet-host stars that have stellar parameters derived by our team in a homogeneous way. In the top panels we show the planet host counts by separating the population of high-mass planets (HMP; 700 planets, with minimum masses greater than $30 M_{\oplus}$) and LMPs (156 planets). The location of the gap in the planet mass distribution presented in Mayor et al. (2011) is $30 M_{\oplus}$ and we also keep this threshold to be consistent with our previous works (e.g., Sousa et al. 2011b). In this work, the metallicity of the host star appears multiple times for systems with multiple planets. On the bottom panels we plot the metallicity distribution of the planet-hosting stars. The planet with the highest minimum mass is considered for multiplanet systems. Three different population of stars are represented: *i*) high-mass planet hosts (HMPH; 600 stars, i.e., planet-host stars that have at least one orbiting planet with a minimum mass greater than $30 M_{\oplus}$); *ii*) low-mass planet hosts (LMPH; 61 stars); and *iii*) a sample of 1111 stars located in the solar neighborhood taken from the HARPS sample discussed in Adibekyan et al. (2012). We note that about 15% of the solar neighborhood sample stars are known to host planets. Our goal is not to compare with nonhost stars, but to compare with the general distribution of stars.

Both cases (planet counts, and planet host counts) are represented in Fig. 4 where we show the metallicity distribution of the different populations in the left panels and in the right panels we present the cumulative distribution function (CDF) of the distributions that allow us to better compare the different distributions.

As expected, the increasing number of exoplanets continues to reinforce the metallicity correlation observed for massive planets, while for the LMP the distribution is clearly different, especially when we compare the LMPH with the neighborhood stars, where the resemblances are remarkable and using Kolmogorov-Smirnov (K-S) test we cannot clearly distinct these stars. Just for comparison, in Sousa et al. (2011b) we had only 10 planet-host stars with exo-Neptunes, while we are considering 61 planet-host stars. Table 3 shows the statistics and p-values of the different populations comparisons that we discuss in this work.

Given the similarities between the metallicity distributions of LMPs and the neighborhood stars, and assuming that all these LMPs are included in stars in the solar neighborhood (which is not far from reality since most of these planet-host stars are bright stars observed by RV follow up), this would of course lead to a flat distribution of the LMP frequency in the solar neighborhood as already shown in our previous works (Sousa et al. 2008, 2011b).

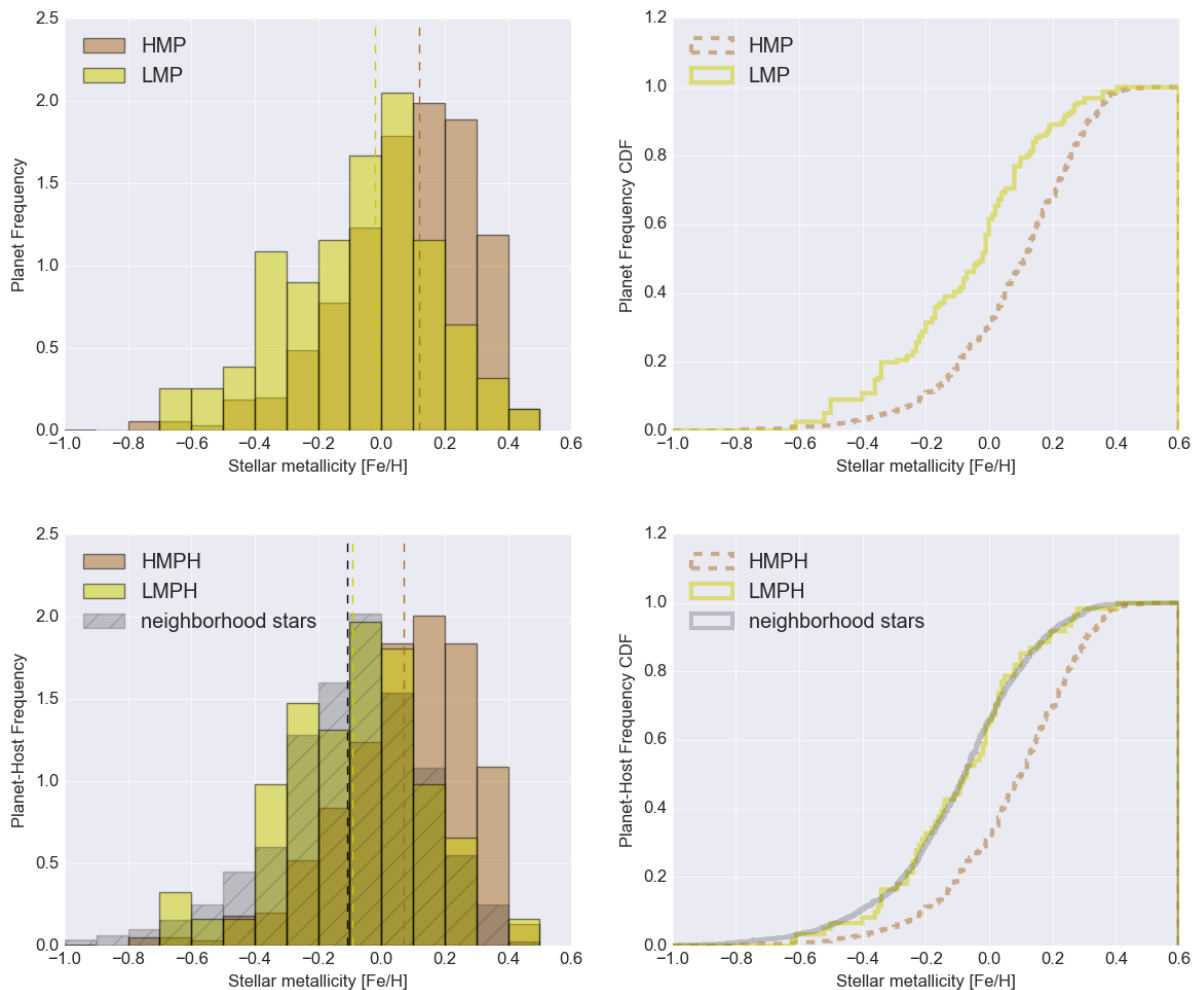


Fig. 4. Metallicity distributions for the HMP and LMP samples (top panel - per planet), and HMPH, LMPH, and a sample representing neighborhood stars (bottom panel - per star). The dashed vertical lines represent the average of each distribution. The right panels shows the CDF for a better comparison.

Table 3. Kolmogorov-Smirnov test comparing the metallicities distribution.

[Fe/H] Samples	K-S statistic	K-S p-value
HMP vs. LMP (1)	0.31	1.82e-11
HMPH vs. LMPH (2)	0.37	2.49e-07
LMPH vs. stars (2)	0.06	9.68e-01

Notes. (1) - Using planet counts; (2) - Using star counts. (see Fig. 4); "stars" corresponds to the solar neighborhood sample.

5. Summary

In this work we update SWEET-Cat with new precise and homogeneous spectroscopic parameters using spectra that we collected from different sources. We describe in detail all the sources of our spectroscopic data used to compile this catalog.

We also update some of the previous stellar parameters listed in the catalog where we confirm the consistency of our results. The new homogeneous parameters are also compared with literature values showing generally good agreement, but with a significant improvement for several specific host stars. We demon-

strate in this work that our spectroscopic analysis method to derive stellar parameters provides very consistent results when analyzing the same stars with many different high-resolution spectrographs.

Finally the known planet-host metallicity correlations are reviewed focusing on the differences found between stars hosting LMPs and stars hosting massive planets. While the giant planet hosts have the clear metallicity correlation, we show that the stars hosting LMPs (with a minimum mass below $30 M_{\oplus}$) are indistinguishable from the solar neighborhood.

Acknowledgements. This work was financed by FEDER - Fundo Europeu de Desenvolvimento Regional funds through the COMPETE 2020 - Operacional Programme for Competitiveness and Internationalisation (POCI), and by Portuguese funds through FCT - Fundação para a Ciência e a Tecnologia in the framework of the projects POCI-01-0145-FEDER-028953, PTDC/FIS-AST/7073/2014 & POCI-01-0145-FEDER-016880, and PTDC/FIS-AST/1526/2014 & POCI-01-0145-FEDER-016886. P.F., S.C.C.B., N.C.S., S.G.S., V.A. and E.D.M. acknowledge support from FCT through Investigador FCT contracts nr. IF/01037/2013CP1191/CT0001, IF/01312/2014/CP1215/CT0004, IF/00169/2012/CP0150/CT0002, IF/00028/2014/CP1215/CT0002, IF/00650/2015/CP1273/CT0001, and IF/00849/2015/CP1273/CT0003. S.G.S. further acknowledges support from FCT in the form of an exploratory project of reference IF/00028/2014/CP1215/CT0002. ACSF is supported by grant 234989/2014-9 from CNPq (Brazil). J.P.F. and acknowledges support from FCT through the grants SFRH/BD/93848/2013 and SFRH/BPD/87857/2012.

B.R.-A. acknowledges the support from CONICYT PAI/Concurso Nacional Inserción en la Academia, Convocatoria 2015 79150050.

References

- Adibekyan, V., Delgado-Mena, E., Figueira, P., et al. 2016, *A&A*, 591, A34
- Adibekyan, V. Z., Figueira, P., Santos, N. C., et al. 2013, *A&A*, 560, A51
- Adibekyan, V. Z., Sousa, S. G., Santos, N. C., et al. 2012, *A&A*, 545, A32
- Ammler-von Eiff, M., Santos, N. C., Sousa, S. G., et al. 2009, *A&A*, 507, 523
- Andreasen, D. T., Sousa, S. G., Tsantaki, M., et al. 2017, *A&A*, 600, A69
- Bean, J. L., Désert, J.-M., Kabath, P., et al. 2011, *ApJ*, 743, 92
- Beaugé, C. & Nesvorný, D. 2013, *ApJ*, 763, 12
- Bedell, M., Meléndez, J., Bean, J. L., et al. 2014, *ApJ*, 795, 23
- Boisse, I., Egeberger, A., Santos, N. C., et al. 2010, *A&A*, 523, A88
- Boisse, I., Pepe, F., Perrier, C., et al. 2012, *A&A*, 545, A55
- Bonomo, A. S., Hébrard, G., Santerne, A., et al. 2012, *A&A*, 538, A96
- Borucki, W. J., Koch, D., Basri, G., et al. 2010, *Science*, 327, 977
- Bouchy, F., Pont, F., Santos, N. C., et al. 2004, *A&A*, 421, L13
- Buchhave, L. A., Bizzarro, M., Latham, D. W., et al. 2014, *Nature*, 509, 593
- Buchhave, L. A. & Latham, D. W. 2015, *ApJ*, 808, 187
- Buchhave, L. A., Latham, D. W., Johansen, A., et al. 2012, *Nature*, 486, 375
- da Silva, R., Udry, S., Bouchy, F., et al. 2007, *A&A*, 473, 323
- Damasso, M., Biazzo, K., Bonomo, A. S., et al. 2015, *A&A*, 575, A111
- Dawson, R. I., Chiang, E., & Lee, E. J. 2015, *MNRAS*, 453, 1471
- Dekker, H., D'Odorico, S., Kaufer, A., Delabre, B., & Kotzlowski, H. 2000, in *Society of Photo-Optical Instrumentation Engineers (SPIE) Conference Series*, Vol. 4008, *Optical and IR Telescope Instrumentation and Detectors*, ed. M. Iye & A. F. Moorwood, 534–545
- Delgado Mena, E., Israelian, G., González Hernández, J. I., et al. 2014, *A&A*, 562, A92
- Díaz, R. F., Rey, J., Demangeon, O., et al. 2016, *A&A*, 591, A146
- Díaz, R. F., Santerne, A., Sahlmann, J., et al. 2012, *A&A*, 538, A113
- Fischer, D. A. & Valenti, J. 2005, *ApJ*, 622, 1102
- Fortier, A., Beck, T., Benz, W., et al. 2014, in *Proc. SPIE*, Vol. 9143, *Space Telescopes and Instrumentation 2014: Optical, Infrared, and Millimeter Wave*, 91432J
- Freudling, W., Romaniello, M., Bramich, D. M., et al. 2013, *A&A*, 559, A96
- Ghezzi, L., Cunha, K., Smith, V. V., et al. 2010, *ApJ*, 720, 1290
- Gillon, M., Pont, F., Moutou, C., et al. 2007, *A&A*, 466, 743
- Gómez Maqueo Chew, Y., Faedi, F., Cargile, P., et al. 2013, *ApJ*, 768, 79
- Hébrard, G., Arnold, L., Forveille, T., et al. 2016, *A&A*, 588, A145
- Hébrard, G., Bonfils, X., Ségransan, D., et al. 2010, *A&A*, 513, A69
- Kurucz, R. 1993, *ATLAS9 Stellar Atmosphere Programs and 2 km/s grid*. Kurucz CD-ROM No. 13. Cambridge, Mass.: Smithsonian Astrophysical Observatory, 1993., 13
- Lillo-Box, J., Demangeon, O., Santerne, A., et al. 2016, *A&A*, 594, A50
- Mayor, M., Marmier, M., Lovis, C., et al. 2011, *ArXiv e-prints* [[arXiv:1109.2497](https://arxiv.org/abs/1109.2497)]
- Mayor, M. & Queloz, D. 1995, *Nature*, 378, 355
- Melo, C., Santos, N. C., Gieren, W., et al. 2007, *A&A*, 467, 721
- Montalto, M., Gregorio, J., Boué, G., et al. 2012, *MNRAS*, 427, 2757
- Mortier, A., Santos, N. C., Sousa, S. G., et al. 2013a, *A&A*, 557, A70
- Mortier, A., Santos, N. C., Sousa, S. G., et al. 2013b, *A&A*, 558, A106
- Mortier, A., Sousa, S. G., Adibekyan, V. Z., Brandão, I. M., & Santos, N. C. 2014, *A&A*, 572, A95
- Moutou, C., Hébrard, G., Bouchy, F., et al. 2014, *A&A*, 563, A22
- Moutou, C., Lo Curto, G., Mayor, M., et al. 2015, *A&A*, 576, A48
- Moutou, C., Loeillet, B., Bouchy, F., et al. 2006, *A&A*, 458, 327
- Moutou, C., Mayor, M., Lo Curto, G., et al. 2011, *A&A*, 527, A63+
- Mulders, G. D., Pascucci, I., Apai, D., Frasca, A., & Molenda-Žakowicz, J. 2016, *AJ*, 152, 187
- Neves, V., Bonfils, X., Santos, N. C., et al. 2013, *A&A*, 551, A36
- Neves, V., Bonfils, X., Santos, N. C., et al. 2014, *A&A*, 568, A121
- Osborn, H. P., Santerne, A., Barros, S. C. C., et al. 2017, *A&A*, 604, A19
- Pont, F., Tamuz, O., Udalski, A., et al. 2008, *A&A*, 487, 749
- Rauer, H., Catala, C., Aerts, C., et al. 2014, *Experimental Astronomy*, 38, 249
- Rey, J., Hébrard, G., Bouchy, F., et al. 2017, *A&A*, 601, A9
- Sahlmann, J., Ségransan, D., Queloz, D., et al. 2011, *A&A*, 525, A95
- Santerne, A., Hébrard, G., Deleuil, M., et al. 2014, *A&A*, 571, A37
- Santerne, A., Hébrard, G., Lillo-Box, J., et al. 2016, *ApJ*, 824, 55
- Santos, N. C., Israelian, G., & Mayor, M. 2004, *A&A*, 415, 1153
- Santos, N. C., Israelian, G., Mayor, M., et al. 2005, *A&A*, 437, 1127
- Santos, N. C., Pont, F., Melo, C., et al. 2006, *A&A*, 450, 825
- Santos, N. C., Sousa, S. G., Mortier, A., et al. 2013, *A&A*, 556, A150
- Santos, N. C., Udry, S., Bouchy, F., et al. 2008, *A&A*, 487, 369
- Schlaufman, K. C. 2015, *ApJ*, 799, L26
- Schlaufman, K. C. & Laughlin, G. 2011, *ApJ*, 738, 177
- Schneider, J., Dedieu, C., Le Sidaner, P., Savalle, R., & Zolotukhin, I. 2011, *A&A*, 532, A79
- Ségransan, D., Udry, S., Mayor, M., et al. 2010, *A&A*, 511, A45
- Snedden, C. 1973, Ph.D. Thesis, Univ. of Texas
- Sousa, S. G. 2014, *ArXiv e-prints* - <http://arxiv.org/abs/1407.5817> [[arXiv:1407.5817](https://arxiv.org/abs/1407.5817)]
- Sousa, S. G., Santos, N. C., Adibekyan, V., Delgado-Mena, E., & Israelian, G. 2015a, *A&A*, 577, A67
- Sousa, S. G., Santos, N. C., Israelian, G., et al. 2011a, *A&A*, 526, A99+
- Sousa, S. G., Santos, N. C., Israelian, G., Mayor, M., & Monteiro, M. J. P. F. G. 2006, *A&A*, 458, 873
- Sousa, S. G., Santos, N. C., Israelian, G., Mayor, M., & Monteiro, M. J. P. F. G. 2007, *A&A*, 469, 783
- Sousa, S. G., Santos, N. C., Israelian, G., Mayor, M., & Udry, S. 2011b, *A&A*, 533, A141
- Sousa, S. G., Santos, N. C., Mayor, M., et al. 2008, *A&A*, 487, 373
- Sousa, S. G., Santos, N. C., Mortier, A., et al. 2015b, *A&A*, 576, A94
- Southworth, J. 2009, *MNRAS*, 394, 272
- Tamuz, O., Ségransan, D., Udry, S., et al. 2008, *A&A*, 480, L33
- Torres, G., Andersen, J., & Giménez, A. 2010, *A&A Rev.*, 18, 67
- Torres, G., Fischer, D. A., Sozzetti, A., et al. 2012, *ApJ*, 757, 161
- Tsantaki, M., Sousa, S. G., Adibekyan, V. Z., et al. 2013, *A&A*, 555, A150
- Tsantaki, M., Sousa, S. G., Santos, N. C., et al. 2014, *A&A*, 570, A80
- Udalski, A., Pont, F., Naef, D., et al. 2008, *A&A*, 482, 299
- Udry, S., Mayor, M., Benz, W., et al. 2006, *A&A*, 447, 361
- Valenti, J. A. & Fischer, D. A. 2005, *ApJS*, 159, 141
- Wagner, F. W., Sohl, F., Hussmann, H., Grott, M., & Rauer, H. 2011, *Icarus*, 214, 366
- Wang, J. & Fischer, D. A. 2015, *AJ*, 149, 14
- Wilson, P. A., Hébrard, G., Santos, N. C., et al. 2016, *A&A*, 588, A144
- Wilson, R. F., Teske, J., Majewski, S. R., et al. 2018, *AJ*, 155, 68
- Zhu, W., Wang, J., & Huang, C. 2016, *ApJ*, 832, 196

Table 4. Spectroscopic Parameters with ARES+MOOG

Star ID	T_{eff} [K]	$\log g_{\text{spec}}$ [cm s ⁻²]	ξ_t [km s ⁻¹]	[Fe/H] [dex]	N(Fe I, Fe II)	Mass [M_{\odot}]	Instrument	SW
BD-061339	4559 ± 281	4.50 ± 0.69	0.57 ± 1.03	-0.34 ± 0.08	94, 6	0.72 ± 0.21	HARPS	yes
BD+152940	4838 ± 46	2.72 ± 0.12	1.43 ± 0.04	-0.15 ± 0.03	82, 9	2.07 ± 0.25	UVES	yes
BD+20594	5659 ± 18	4.28 ± 0.03	0.87 ± 0.03	-0.14 ± 0.01	243, 31	0.95 ± 0.07	HARPS	yes
CoRoT-19	6425 ± 95	4.54 ± 0.09	1.52 ± 0.13	0.24 ± 0.07	215, 29	1.25 ± 0.09	HARPS	yes
CoRoT-25	6166 ± 38	4.41 ± 0.04	1.37 ± 0.05	0.16 ± 0.03	194, 23	1.16 ± 0.08	UVES	yes
CoRoT-6	6278 ± 73	4.76 ± 0.07	1.43 ± 0.14	-0.05 ± 0.05	170, 22	1.05 ± 0.08	UVES	yes
EPIC201295312	5883 ± 29	4.20 ± 0.04	1.15 ± 0.03	0.20 ± 0.02	240, 31	1.17 ± 0.08	HARPS	yes
K2-19	5355 ± 35	4.46 ± 0.06	0.80 ± 0.06	0.05 ± 0.02	230, 33	0.86 ± 0.06	HARPS	yes
K2-24	5706 ± 33	4.36 ± 0.06	1.01 ± 0.04	0.41 ± 0.03	239, 33	1.09 ± 0.08	HARPS	yes
K2-32	5276 ± 37	4.38 ± 0.06	0.66 ± 0.07	-0.05 ± 0.03	245, 34	0.84 ± 0.06	HARPS	yes
etaCet	4687 ± 85	2.63 ± 0.21	1.41 ± 0.08	0.15 ± 0.05	79, 10	2.25 ± 0.44	UVES	yes
GJ160.2	4498 ± 152	4.35 ± 0.50	0.15 ± 1.40	-0.26 ± 0.08	94, 6	0.70 ± 0.14	HARPS	yes
HAT-P-13	5797 ± 34	4.14 ± 0.06	1.03 ± 0.04	0.44 ± 0.03	231, 32	1.27 ± 0.09	SOPHIE	yes
HAT-P-45	6394 ± 94	4.58 ± 0.08	1.38 ± 0.14	0.01 ± 0.07	169, 21	1.14 ± 0.08	UVES	yes
HAT-P-50	6283 ± 82	4.17 ± 0.11	1.63 ± 0.13	-0.11 ± 0.06	166, 21	1.23 ± 0.10	UVES	yes
HAT-P-54	4505 ± 163	4.22 ± 0.56	0.91 ± 0.38	-0.04 ± 0.06	83, 8	0.75 ± 0.20	UVES	yes
HATS-13	5526 ± 71	4.62 ± 0.12	1.00 ± 0.12	0.10 ± 0.05	228, 34	0.89 ± 0.07	FEROS	yes
HATS-2	5233 ± 99	4.45 ± 0.19	1.62 ± 0.12	0.22 ± 0.05	213, 32	0.88 ± 0.08	FEROS	yes
HD113337	6918 ± 47	4.71 ± 0.07	1.82 ± 0.07	0.25 ± 0.03	214, 34	1.38 ± 0.09	SOPHIE	yes
HD128356	4932 ± 126	4.31 ± 0.29	0.64 ± 0.25	0.25 ± 0.06	109, 14	0.84 ± 0.11	HARPS	yes
HD14067	4883 ± 49	2.76 ± 0.11	1.52 ± 0.05	-0.08 ± 0.04	87, 11	2.07 ± 0.23	UVES	yes
HD141399	5602 ± 34	4.24 ± 0.05	0.90 ± 0.05	0.36 ± 0.03	233, 34	1.09 ± 0.08	SOPHIE	yes
HD142245	4843 ± 66	3.21 ± 0.14	1.18 ± 0.07	0.13 ± 0.04	81, 10	1.53 ± 0.20	UVES	yes
HD143761	5829 ± 14	4.29 ± 0.02	1.02 ± 0.02	-0.20 ± 0.01	242, 30	0.98 ± 0.07	SOPHIE	yes
HD147873	6191 ± 30	4.14 ± 0.04	1.71 ± 0.04	0.24 ± 0.02	237, 32	1.35 ± 0.09	HARPS	yes
HD155233	4842 ± 45	3.16 ± 0.12	1.16 ± 0.04	0.06 ± 0.03	112, 15	1.57 ± 0.18	FEROS	yes
HD156668	4804 ± 141	4.44 ± 0.33	0.42 ± 0.57	-0.02 ± 0.06	90, 9	0.75 ± 0.10	UVES	yes
HD162004	6273 ± 33	4.50 ± 0.04	1.23 ± 0.04	0.08 ± 0.02	219, 30	1.14 ± 0.08	SOPHIE	yes
HD164595	5725 ± 14	4.41 ± 0.03	0.90 ± 0.03	-0.09 ± 0.01	242, 32	0.94 ± 0.07	SOPHIE	yes
HD165155	5387 ± 31	4.39 ± 0.05	0.81 ± 0.05	0.12 ± 0.02	237, 33	0.90 ± 0.07	HARPS	yes
HD1666	6510 ± 55	4.25 ± 0.06	1.77 ± 0.07	0.39 ± 0.04	224, 29	1.44 ± 0.10	HARPS	yes
HD1666	6497 ± 35	4.20 ± 0.06	1.67 ± 0.04	0.38 ± 0.03	187, 22	1.46 ± 0.10	UVES	no
HD189733	5080 ± 91	4.51 ± 0.20	0.74 ± 0.17	-0.02 ± 0.04	95, 13	0.79 ± 0.07	CORALIE	no
HD189733	4984 ± 59	4.40 ± 0.13	0.68 ± 0.14	-0.04 ± 0.03	115, 13	0.78 ± 0.06	ESPADONS	no
HD189733	5010 ± 48	4.44 ± 0.12	0.83 ± 0.10	-0.05 ± 0.02	112, 12	0.77 ± 0.06	FEROS	no
HD189733	4969 ± 43	4.31 ± 0.10	0.76 ± 0.10	-0.07 ± 0.02	114, 14	0.78 ± 0.06	HARPS	yes
HD222076	4834 ± 59	3.24 ± 0.13	1.15 ± 0.06	0.16 ± 0.03	112, 13	1.50 ± 0.18	FEROS	yes
HD224538	6235 ± 24	4.37 ± 0.04	1.34 ± 0.03	0.37 ± 0.02	247, 34	1.30 ± 0.09	HARPS	yes
HD32963	5789 ± 33	4.46 ± 0.05	1.01 ± 0.05	0.12 ± 0.03	231, 32	1.00 ± 0.07	FEROS	no
HD32963	5767 ± 23	4.38 ± 0.03	0.83 ± 0.04	0.09 ± 0.02	235, 32	1.01 ± 0.07	SOPHIE	yes
HD33844	4832 ± 63	3.01 ± 0.14	1.21 ± 0.06	0.18 ± 0.04	110, 14	1.79 ± 0.24	FEROS	yes
HD42618	5751 ± 11	4.45 ± 0.01	0.94 ± 0.02	-0.09 ± 0.01	246, 29	0.94 ± 0.07	HARPS	yes
HD42618	5736 ± 16	4.44 ± 0.03	0.85 ± 0.03	-0.11 ± 0.01	243, 31	0.93 ± 0.07	SOPHIE	no
HD47366	4919 ± 37	3.08 ± 0.08	1.26 ± 0.04	-0.00 ± 0.03	114, 14	1.67 ± 0.15	HARPS	yes
HD47366	4914 ± 42	3.06 ± 0.09	1.24 ± 0.04	0.01 ± 0.03	89, 11	1.69 ± 0.16	UVES	no
HD4747	5333 ± 23	4.45 ± 0.06	0.76 ± 0.05	-0.21 ± 0.02	241, 30	0.81 ± 0.06	FEROS	yes
HD68402	5907 ± 33	4.43 ± 0.04	1.04 ± 0.04	0.27 ± 0.03	238, 31	1.10 ± 0.08	HARPS	yes
HD72892	5685 ± 29	4.33 ± 0.04	0.95 ± 0.04	0.15 ± 0.02	239, 33	1.02 ± 0.07	HARPS	yes
HD9174	5631 ± 30	4.05 ± 0.04	1.12 ± 0.03	0.36 ± 0.02	243, 33	1.22 ± 0.08	HARPS	yes
HD95872	5304 ± 71	4.41 ± 0.13	0.92 ± 0.10	0.26 ± 0.04	172, 24	0.91 ± 0.08	UVES	yes
HIP105854	4575 ± 102	2.43 ± 0.27	1.47 ± 0.09	0.21 ± 0.05	102, 14	2.56 ± 0.63	FEROS	no
HIP105854	4618 ± 113	2.36 ± 0.28	1.47 ± 0.11	0.17 ± 0.07	74, 10	2.74 ± 0.73	UVES	yes
HIP63242	4812 ± 37	2.51 ± 0.09	1.68 ± 0.04	-0.31 ± 0.03	113, 12	2.32 ± 0.23	FEROS	yes
HIP65891	4928 ± 43	2.89 ± 0.12	1.38 ± 0.04	0.12 ± 0.03	108, 14	1.98 ± 0.24	FEROS	yes
HIP67537	4976 ± 46	2.95 ± 0.11	1.40 ± 0.04	0.17 ± 0.03	109, 14	1.95 ± 0.22	FEROS	yes
HIP67851	4805 ± 39	3.19 ± 0.14	1.13 ± 0.05	0.01 ± 0.03	112, 14	1.49 ± 0.19	FEROS	no
HIP67851	4809 ± 51	3.09 ± 0.12	1.11 ± 0.06	-0.01 ± 0.03	88, 11	1.60 ± 0.18	UVES	yes
HIP68468	5840 ± 12	4.34 ± 0.01	1.08 ± 0.02	0.08 ± 0.01	240, 32	1.04 ± 0.07	HARPS	yes
HIP74890	4808 ± 69	3.09 ± 0.17	1.24 ± 0.07	0.21 ± 0.04	109, 15	1.68 ± 0.25	FEROS	no

Table 4. continued.

Star ID	T_{eff} [K]	$\log g_{\text{spec}}$ [cm s^{-2}]	ξ_t [km s^{-1}]	[Fe/H] [dex]	N(Fe I, Fe II)	Mass [M_{\odot}]	Instrument	SW
HIP74890	4848 ± 84	3.33 ± 0.20	1.28 ± 0.10	0.20 ± 0.05	85, 11	1.45 ± 0.23	UVES	yes
HIP8541	4616 ± 46	2.89 ± 0.13	1.18 ± 0.04	-0.08 ± 0.02	112, 14	1.71 ± 0.21	FEROS	yes
HIP97233	4955 ± 60	3.24 ± 0.14	1.24 ± 0.06	0.27 ± 0.04	111, 14	1.61 ± 0.20	FEROS	yes
K2-31	5406 ± 33	4.43 ± 0.06	0.95 ± 0.07	0.16 ± 0.02	235, 31	0.91 ± 0.07	HARPS	yes
KELT-10	5850 ± 37	4.40 ± 0.04	1.05 ± 0.05	0.13 ± 0.03	196, 21	1.04 ± 0.07	UVES	yes
KELT-15	6428 ± 72	4.58 ± 0.08	1.77 ± 0.09	0.24 ± 0.05	162, 20	1.24 ± 0.09	UVES	yes
KELT-8	5804 ± 37	4.32 ± 0.06	1.16 ± 0.05	0.25 ± 0.03	198, 24	1.09 ± 0.08	UVES	yes
Kepler-10	5685 ± 27	4.35 ± 0.04	0.64 ± 0.05	-0.14 ± 0.02	240, 29	0.93 ± 0.07	SOPHIE	yes
Kepler-68	5884 ± 45	4.35 ± 0.09	0.99 ± 0.06	0.15 ± 0.04	227, 32	1.08 ± 0.08	SOPHIE	yes
Kepler-93	5624 ± 40	4.48 ± 0.08	0.72 ± 0.08	-0.15 ± 0.03	226, 28	0.89 ± 0.07	SOPHIE	yes
Pr0201	6247 ± 46	4.51 ± 0.06	1.40 ± 0.06	0.25 ± 0.03	187, 24	1.19 ± 0.08	UVES	yes
WASP-101	6503 ± 100	4.68 ± 0.11	1.81 ± 0.17	0.18 ± 0.07	210, 31	1.22 ± 0.09	HARPS	yes
WASP-101	6534 ± 132	4.89 ± 0.11	1.78 ± 0.23	0.18 ± 0.09	152, 19	1.23 ± 0.09	UVES	no
WASP-104	5416 ± 86	4.36 ± 0.16	0.76 ± 0.16	0.40 ± 0.06	187, 25	0.99 ± 0.09	UVES	yes
WASP-105	5183 ± 66	4.23 ± 0.16	0.72 ± 0.14	0.36 ± 0.04	111, 15	0.95 ± 0.09	HARPS	yes
WASP-106	6265 ± 36	4.38 ± 0.04	1.39 ± 0.04	0.15 ± 0.03	225, 32	1.21 ± 0.08	HARPS	yes
WASP-108	6193 ± 33	4.47 ± 0.04	1.27 ± 0.04	0.26 ± 0.02	189, 23	1.18 ± 0.08	UVES	yes
WASP-111	6698 ± 125	4.78 ± 0.09	2.42 ± 0.21	0.25 ± 0.08	155, 20	1.32 ± 0.10	UVES	yes
WASP-117	6026 ± 17	4.35 ± 0.02	1.17 ± 0.03	-0.13 ± 0.01	245, 32	1.04 ± 0.07	HARPS	yes
WASP-122	5859 ± 41	4.31 ± 0.05	1.18 ± 0.05	0.37 ± 0.03	189, 21	1.16 ± 0.08	UVES	yes
WASP-126	5807 ± 39	4.39 ± 0.06	1.09 ± 0.05	0.19 ± 0.03	185, 23	1.05 ± 0.08	UVES	yes
WASP-129	5983 ± 23	4.38 ± 0.04	1.13 ± 0.03	0.16 ± 0.02	234, 32	1.11 ± 0.08	HARPS	yes
WASP-130	5667 ± 34	4.43 ± 0.05	0.96 ± 0.05	0.31 ± 0.03	247, 34	1.02 ± 0.07	HARPS	yes
WASP-131	6143 ± 23	4.18 ± 0.04	1.33 ± 0.03	-0.01 ± 0.02	245, 34	1.20 ± 0.08	HARPS	yes
WASP-132	4742 ± 201	4.23 ± 0.50	0.40 ± 0.86	0.21 ± 0.09	106, 13	0.84 ± 0.21	HARPS	yes
WASP-139	5109 ± 70	4.40 ± 0.15	0.60 ± 0.16	0.05 ± 0.04	111, 14	0.82 ± 0.07	HARPS	yes
WASP-20	5987 ± 20	4.33 ± 0.03	1.19 ± 0.03	0.07 ± 0.02	247, 35	1.09 ± 0.08	HARPS	yes
WASP-39	5512 ± 40	4.36 ± 0.06	0.72 ± 0.07	0.04 ± 0.03	184, 24	0.93 ± 0.07	UVES	yes
WASP-43	4798 ± 216	4.55 ± 0.71	0.98 ± 0.52	-0.13 ± 0.08	65, 6	0.80 ± 0.24	UVES	yes
WASP-46	5725 ± 39	4.47 ± 0.06	0.82 ± 0.07	-0.18 ± 0.03	191, 23	0.91 ± 0.07	UVES	yes
WASP-48	6334 ± 103	4.55 ± 0.15	1.86 ± 0.17	-0.02 ± 0.07	194, 25	1.12 ± 0.09	SOPHIE	yes
WASP-49	5540 ± 18	4.36 ± 0.03	0.82 ± 0.03	-0.07 ± 0.01	247, 31	0.91 ± 0.06	HARPS	yes
WASP-49	5534 ± 28	4.31 ± 0.04	0.80 ± 0.05	-0.08 ± 0.02	195, 23	0.92 ± 0.07	UVES	no
WASP-68	5985 ± 21	4.19 ± 0.03	1.29 ± 0.02	0.34 ± 0.02	236, 32	1.28 ± 0.08	HARPS	yes
WASP-69	4765 ± 120	4.13 ± 0.31	0.79 ± 0.30	0.30 ± 0.06	105, 15	0.86 ± 0.14	HARPS	yes
WASP-70A	5864 ± 25	4.36 ± 0.03	1.01 ± 0.03	0.21 ± 0.02	191, 24	1.09 ± 0.07	UVES	yes
WASP-74	6075 ± 43	4.43 ± 0.06	1.26 ± 0.05	0.48 ± 0.03	200, 23	1.24 ± 0.08	UVES	yes
WASP-90	6339 ± 65	4.28 ± 0.04	1.58 ± 0.08	0.14 ± 0.05	168, 23	1.29 ± 0.09	UVES	yes
XO-4	6707 ± 86	4.79 ± 0.07	1.87 ± 0.14	0.02 ± 0.05	198, 31	1.22 ± 0.09	SOPHIE	yes
YBP1194	5970 ± 26	4.42 ± 0.05	1.13 ± 0.03	-0.00 ± 0.02	192, 23	1.03 ± 0.07	UVES	yes
YBP1514	5076 ± 34	3.61 ± 0.09	0.98 ± 0.04	0.09 ± 0.02	91, 10	1.23 ± 0.11	UVES	yes
YBP401	6131 ± 37	4.36 ± 0.04	1.13 ± 0.05	0.04 ± 0.03	238, 33	1.13 ± 0.08	HARPS	yes

Table 5. Spectroscopic Parameters with synthesis

Star ID	T_{eff} [K]	$\log g_{\text{spec}}$ [cm s^{-2}]	v_{mic} [km s^{-1}]	[Fe/H] [dex]	$v \sin(i)$ [km s^{-1}]	v_{mac} [km s^{-1}]	Mass [M_{\odot}]	Instrument	SW
38Vir	6440 ± 51	4.42 ± 0.22	1.44	0.16 ± 0.05	28.10 ± 1.30	4.92	1.29 ± 0.12	HARPS	yes
EPIC211990866	5981 ± 44	4.32 ± 0.15	1.19	0.18 ± 0.04	13.60 ± 0.30	4.19	1.15 ± 0.10	UVES	yes
HAT-P-56	6491 ± 72	4.26 ± 0.30	1.73	-0.22 ± 0.03	33.60 ± 1.30	4.82	1.25 ± 0.16	UVES	yes
WASP-103	6013 ± 44	4.24 ± 0.15	1.17	0.08 ± 0.04	10.10 ± 0.30	3.82	1.16 ± 0.10	FIES	yes
WASP-109	6573 ± 44	3.94 ± 0.15	1.76	-0.10 ± 0.04	15.70 ± 0.30	5.20	1.49 ± 0.15	UVES	yes
WASP-120	6657 ± 44	4.41 ± 0.15	1.63	0.15 ± 0.04	15.00 ± 0.30	5.27	1.35 ± 0.10	UVES	yes
WASP-87A	6638 ± 44	4.06 ± 0.15	1.73	-0.21 ± 0.04	10.40 ± 0.30	4.82	1.39 ± 0.13	UVES	yes
Aldebaran	3999 ± 25	1.67 ± 0.09	2.24	-0.24 ± 0.03	2.50 ± 0.60	6.05	3.28 ± 0.31	UVES	yes
betaCnc	4077 ± 25	1.34 ± 0.09	2.04	-0.30 ± 0.03	0.20 ± 0.10	6.32	4.19 ± 0.37	UVES	yes
HIP70849	4103 ± 25	3.70 ± 0.09	0.10	0.00 ± 0.03	0.30 ± 0.30	6.17	0.76 ± 0.07	HARPS	yes
HD208527	4118 ± 25	1.83 ± 0.09	2.44	0.15 ± 0.03	5.90 ± 0.60	5.98	3.37 ± 0.33	UVES	yes

Table 6. Spectroscopic Parameters with ARES+MOOG for old data.

Star ID	T_{eff} [K]	$\log g_{\text{spec}}$ [cm s^{-2}]	ξ_t [km s^{-1}]	[Fe/H] [dex]	N(Fe I, Fe II)	Mass [M_{\odot}]	Instrument	SW
14Her	5452 ± 55	4.31 ± 0.16	1.10 ± 0.10	0.39 ± 0.04	196, 25	1.02 ± 0.09	ELODIE	no
14Her	5368 ± 94	4.33 ± 0.15	0.92 ± 0.14	0.44 ± 0.06	214, 27	1.00 ± 0.09	SARG	no
14Her	5286 ± 58	4.24 ± 0.11	0.80 ± 0.09	0.38 ± 0.04	222, 35	0.98 ± 0.08	SOPHIE	yes
16CygB	5827 ± 39	4.30 ± 0.06	0.97 ± 0.05	0.14 ± 0.03	217, 27	1.07 ± 0.08	ELODIE	no
16CygB	5783 ± 19	4.42 ± 0.03	0.96 ± 0.03	0.09 ± 0.01	248, 33	1.00 ± 0.07	ESPADONS	yes
16CygB	5785 ± 28	4.41 ± 0.04	1.02 ± 0.04	0.10 ± 0.02	226, 28	1.01 ± 0.07	SARG	no
51Peg	5854 ± 24	4.36 ± 0.04	1.10 ± 0.03	0.26 ± 0.02	229, 26	1.10 ± 0.08	FEROS	no
51Peg	5814 ± 19	4.35 ± 0.03	1.04 ± 0.03	0.21 ± 0.01	197, 24	1.07 ± 0.07	UVES	yes
55Cnc	5346 ± 80	4.26 ± 0.18	1.29 ± 0.10	0.25 ± 0.05	207, 23	0.97 ± 0.10	ELODIE	no
55Cnc	5353 ± 62	4.30 ± 0.14	1.01 ± 0.10	0.30 ± 0.04	183, 25	0.97 ± 0.08	UVES	yes
61Vir	5569 ± 24	4.39 ± 0.04	0.84 ± 0.04	0.03 ± 0.02	249, 33	0.93 ± 0.07	FEROS	no
61Vir	5559 ± 17	4.36 ± 0.03	0.80 ± 0.03	-0.01 ± 0.01	244, 31	0.93 ± 0.07	HARPS	yes
61Vir	5580 ± 21	4.39 ± 0.03	0.82 ± 0.04	0.02 ± 0.02	242, 28	0.93 ± 0.07	NARVAL	no
61Vir	5556 ± 15	4.35 ± 0.03	0.84 ± 0.03	-0.02 ± 0.01	197, 22	0.93 ± 0.07	UVES	no
70Vir	5568 ± 29	4.00 ± 0.06	1.00 ± 0.04	-0.02 ± 0.02	213, 22	1.09 ± 0.08	ELODIE	no
70Vir	5565 ± 25	4.05 ± 0.05	1.05 ± 0.03	-0.03 ± 0.02	234, 27	1.05 ± 0.08	SARG	yes
BD-103166	5367 ± 56	4.36 ± 0.12	1.02 ± 0.08	0.30 ± 0.04	222, 30	0.95 ± 0.08	FEROS	yes
GJ3021	5492 ± 37	4.45 ± 0.06	1.16 ± 0.05	0.11 ± 0.03	221, 29	0.91 ± 0.07	CORALIE	no
GJ3021	5557 ± 36	4.47 ± 0.07	1.05 ± 0.06	0.13 ± 0.03	237, 32	0.93 ± 0.07	HARPS	yes
HD102195	5293 ± 34	4.37 ± 0.07	0.93 ± 0.07	0.03 ± 0.02	229, 30	0.86 ± 0.06	ESPADONS	no
HD102195	5311 ± 29	4.44 ± 0.06	0.85 ± 0.05	0.04 ± 0.02	228, 32	0.85 ± 0.06	HARPS	yes
HD106252	5887 ± 25	4.41 ± 0.06	1.09 ± 0.04	-0.04 ± 0.02	237, 24	1.00 ± 0.07	FEROS	no
HD106252	5871 ± 15	4.38 ± 0.03	1.10 ± 0.02	-0.07 ± 0.01	200, 23	1.00 ± 0.07	UVES	yes
HD10697	5711 ± 39	4.15 ± 0.04	1.23 ± 0.04	0.16 ± 0.03	236, 28	1.11 ± 0.08	SARG	no
HD10697	5653 ± 21	4.01 ± 0.03	1.06 ± 0.03	0.13 ± 0.02	234, 33	1.17 ± 0.08	SOPHIE	yes
HD108874	5590 ± 60	4.34 ± 0.09	0.91 ± 0.09	0.22 ± 0.04	179, 22	1.00 ± 0.08	UES	yes
HD109749	5885 ± 34	4.30 ± 0.05	1.05 ± 0.04	0.30 ± 0.03	236, 33	1.15 ± 0.08	CORALIE	no
HD109749	5881 ± 22	4.28 ± 0.03	1.11 ± 0.03	0.26 ± 0.02	198, 25	1.15 ± 0.08	UVES	yes
HD114762	5869 ± 34	4.31 ± 0.03	1.03 ± 0.06	-0.65 ± 0.03	201, 30	0.88 ± 0.06	FIES	no
HD114762	5961 ± 26	4.43 ± 0.03	1.35 ± 0.06	-0.65 ± 0.02	158, 21	0.87 ± 0.06	UVES	yes
HD11964	5360 ± 26	3.86 ± 0.06	1.14 ± 0.03	0.10 ± 0.02	233, 29	1.15 ± 0.09	FEROS	no
HD11964	5326 ± 19	3.87 ± 0.04	0.92 ± 0.03	0.10 ± 0.01	239, 32	1.12 ± 0.08	HARPS	yes
HD12661	5775 ± 33	4.36 ± 0.06	1.09 ± 0.04	0.40 ± 0.03	245, 33	1.12 ± 0.08	FEROS	yes
HD12661	5749 ± 37	4.30 ± 0.07	1.10 ± 0.04	0.36 ± 0.03	235, 30	1.12 ± 0.08	UES	no
HD142415	5977 ± 27	4.52 ± 0.05	1.08 ± 0.04	0.17 ± 0.02	249, 33	1.06 ± 0.07	FEROS	yes
HD149143	5971 ± 39	4.21 ± 0.06	1.25 ± 0.04	0.35 ± 0.03	222, 28	1.26 ± 0.09	CORALIE	no
HD149143	5950 ± 21	4.21 ± 0.04	1.25 ± 0.03	0.32 ± 0.02	246, 32	1.24 ± 0.08	ESPADONS	yes
HD150706	5928 ± 22	4.47 ± 0.03	0.97 ± 0.03	-0.03 ± 0.02	247, 29	1.00 ± 0.07	SOPHIE	yes
HD154857	5567 ± 20	3.90 ± 0.03	1.15 ± 0.03	-0.24 ± 0.02	234, 25	1.08 ± 0.08	FEROS	no
HD154857	5560 ± 12	3.90 ± 0.02	1.13 ± 0.02	-0.26 ± 0.01	202, 23	1.07 ± 0.07	UVES	yes
HD168443	5590 ± 17	4.11 ± 0.03	1.05 ± 0.02	0.06 ± 0.01	247, 31	1.06 ± 0.07	HARPS	yes
HD178911B	5644 ± 32	4.38 ± 0.04	0.80 ± 0.06	0.20 ± 0.03	239, 34	1.00 ± 0.07	SOPHIE	yes
HD183263	5938 ± 22	4.32 ± 0.04	1.18 ± 0.03	0.30 ± 0.02	229, 25	1.17 ± 0.08	FEROS	no
HD183263	5986 ± 21	4.39 ± 0.04	1.11 ± 0.03	0.32 ± 0.02	247, 33	1.16 ± 0.08	HARPS	yes
HD185269	5998 ± 43	3.98 ± 0.06	1.42 ± 0.05	0.14 ± 0.03	228, 31	1.35 ± 0.10	ELODIE	yes
HD187123	5835 ± 18	4.38 ± 0.03	1.04 ± 0.02	0.13 ± 0.01	249, 33	1.04 ± 0.07	ESPADONS	yes
HD187123	5877 ± 27	4.50 ± 0.04	1.05 ± 0.04	0.16 ± 0.02	231, 27	1.03 ± 0.07	SARG	no
HD188015	5726 ± 28	4.35 ± 0.06	1.05 ± 0.04	0.27 ± 0.02	224, 23	1.06 ± 0.08	FEROS	yes
HD190228	5301 ± 16	3.79 ± 0.02	0.96 ± 0.02	-0.24 ± 0.01	202, 23	1.05 ± 0.07	UVES	yes
HD190360	5604 ± 28	4.31 ± 0.05	0.96 ± 0.04	0.23 ± 0.02	241, 32	1.02 ± 0.07	ESPADONS	yes
HD190360	5620 ± 39	4.28 ± 0.07	1.02 ± 0.05	0.26 ± 0.03	183, 21	1.05 ± 0.08	UES	no
HD195019	5790 ± 20	4.19 ± 0.04	1.06 ± 0.03	0.09 ± 0.02	213, 28	1.10 ± 0.08	CORALIE	no
HD195019	5800 ± 14	4.21 ± 0.03	1.08 ± 0.02	0.07 ± 0.01	201, 24	1.08 ± 0.07	UVES	yes
HD196885A	6308 ± 55	4.42 ± 0.05	1.59 ± 0.07	0.27 ± 0.04	198, 22	1.26 ± 0.09	SARG	yes
HD2039	5948 ± 39	4.42 ± 0.08	1.01 ± 0.05	0.37 ± 0.03	234, 33	1.15 ± 0.08	CORALIE	no
HD2039	5968 ± 22	4.42 ± 0.03	1.10 ± 0.03	0.33 ± 0.02	196, 24	1.15 ± 0.08	UVES	yes
HD216437	5860 ± 19	4.21 ± 0.03	1.24 ± 0.02	0.24 ± 0.02	199, 25	1.17 ± 0.08	UVES	yes
HD217107	5657 ± 34	4.29 ± 0.07	1.17 ± 0.04	0.34 ± 0.03	232, 26	1.08 ± 0.08	FEROS	no
HD217107	5647 ± 30	4.28 ± 0.05	0.96 ± 0.04	0.34 ± 0.02	188, 24	1.09 ± 0.08	UVES	yes

Table 6. continued.

Star ID	T_{eff} [K]	$\log g_{\text{spec}}$ [cm s^{-2}]	ξ_t [km s^{-1}]	[Fe/H] [dex]	N(Fe I, Fe II)	Mass [M_{\odot}]	Instrument	SW
HD219828	5888 ± 14	4.20 ± 0.02	1.17 ± 0.01	0.18 ± 0.01	242, 32	1.16 ± 0.08	HARPS	yes
HD23596	6099 ± 33	4.30 ± 0.06	1.29 ± 0.04	0.31 ± 0.03	230, 28	1.25 ± 0.09	UES	yes
HD30562	5957 ± 31	4.22 ± 0.04	1.23 ± 0.03	0.26 ± 0.03	226, 32	1.21 ± 0.08	CORALIE	no
HD30562	5945 ± 41	4.10 ± 0.07	1.25 ± 0.05	0.27 ± 0.03	209, 25	1.30 ± 0.09	ELODIE	no
HD30562	5963 ± 24	4.24 ± 0.05	1.28 ± 0.03	0.28 ± 0.02	228, 27	1.21 ± 0.08	FEROS	yes
HD34445	5840 ± 23	4.19 ± 0.04	1.21 ± 0.03	0.13 ± 0.02	224, 27	1.13 ± 0.08	CORALIE	yes
HD37124	5503 ± 32	4.42 ± 0.05	0.62 ± 0.07	-0.41 ± 0.03	238, 30	0.82 ± 0.06	FIES	no
HD37124	5510 ± 16	4.39 ± 0.03	0.84 ± 0.03	-0.43 ± 0.01	190, 21	0.82 ± 0.06	UVES	yes
HD37605	5450 ± 46	4.31 ± 0.10	1.09 ± 0.07	0.28 ± 0.03	232, 31	0.98 ± 0.08	FEROS	yes
HD38529	5628 ± 34	3.81 ± 0.07	1.36 ± 0.04	0.36 ± 0.03	222, 26	1.40 ± 0.11	FEROS	no
HD38529	5653 ± 29	3.83 ± 0.05	1.29 ± 0.03	0.37 ± 0.02	194, 25	1.40 ± 0.10	UVES	yes
HD41004A	5255 ± 52	4.34 ± 0.11	0.97 ± 0.08	0.15 ± 0.03	222, 30	0.89 ± 0.07	FEROS	yes
HD4203	5652 ± 33	4.14 ± 0.08	1.19 ± 0.04	0.39 ± 0.03	219, 25	1.18 ± 0.09	FEROS	no
HD4203	5656 ± 38	4.10 ± 0.06	1.13 ± 0.04	0.38 ± 0.03	189, 24	1.21 ± 0.09	UVES	yes
HD43691	6258 ± 41	4.31 ± 0.07	1.45 ± 0.04	0.32 ± 0.03	221, 29	1.32 ± 0.09	SOPHIE	yes
HD46375	5305 ± 50	4.39 ± 0.09	0.87 ± 0.08	0.23 ± 0.03	232, 34	0.90 ± 0.07	ESPADONS	yes
HD46375	5290 ± 65	4.26 ± 0.12	1.09 ± 0.08	0.17 ± 0.04	229, 27	0.93 ± 0.08	UES	no
HD49674	5662 ± 28	4.42 ± 0.05	0.93 ± 0.04	0.30 ± 0.02	242, 30	1.03 ± 0.07	ESPADONS	yes
HD49674	5674 ± 53	4.49 ± 0.07	0.86 ± 0.09	0.34 ± 0.04	216, 27	1.02 ± 0.07	SARG	no
HD49674	5628 ± 33	4.39 ± 0.05	0.82 ± 0.05	0.27 ± 0.02	242, 33	1.01 ± 0.07	SOPHIE	no
HD50499	6043 ± 34	4.23 ± 0.04	1.31 ± 0.04	0.33 ± 0.03	233, 30	1.27 ± 0.09	CORALIE	no
HD50499	6077 ± 19	4.36 ± 0.04	1.27 ± 0.02	0.34 ± 0.01	248, 33	1.22 ± 0.08	HARPS	yes
HD50554	6061 ± 23	4.47 ± 0.03	1.18 ± 0.03	0.03 ± 0.02	204, 24	1.06 ± 0.07	UVES	no
HD6434	5721 ± 45	4.29 ± 0.04	0.82 ± 0.08	-0.53 ± 0.04	154, 18	0.87 ± 0.06	FEROS	yes
HD68988	5946 ± 64	4.39 ± 0.12	1.35 ± 0.08	0.34 ± 0.05	191, 23	1.16 ± 0.09	SARG	yes
HD73526	5629 ± 32	4.08 ± 0.06	1.12 ± 0.04	0.26 ± 0.03	242, 31	1.16 ± 0.08	FEROS	no
HD73526	5661 ± 25	4.15 ± 0.04	1.10 ± 0.03	0.26 ± 0.02	203, 24	1.13 ± 0.08	UVES	yes
HD74156	6108 ± 30	4.37 ± 0.04	1.29 ± 0.04	0.17 ± 0.02	218, 26	1.16 ± 0.08	FEROS	no
HD74156	6065 ± 21	4.25 ± 0.03	1.28 ± 0.03	0.13 ± 0.02	206, 24	1.18 ± 0.08	UVES	yes
HD76700	5645 ± 29	4.14 ± 0.05	1.12 ± 0.03	0.35 ± 0.02	219, 22	1.16 ± 0.08	FEROS	no
HD76700	5689 ± 29	4.18 ± 0.05	1.06 ± 0.04	0.37 ± 0.02	199, 25	1.16 ± 0.08	UVES	yes
HD80606	5542 ± 36	4.28 ± 0.06	0.79 ± 0.05	0.27 ± 0.03	237, 34	1.02 ± 0.07	SOPHIE	yes
HD80606	5582 ± 81	4.60 ± 0.15	1.03 ± 0.12	0.25 ± 0.06	204, 28	0.95 ± 0.08	UES	no
HD81040	5684 ± 30	4.38 ± 0.04	0.91 ± 0.05	-0.08 ± 0.02	232, 33	0.94 ± 0.07	CORALIE	no
HD81040	5778 ± 23	4.54 ± 0.03	0.88 ± 0.04	-0.03 ± 0.02	246, 31	0.94 ± 0.07	FIES	yes
HD8574	6070 ± 41	4.26 ± 0.05	1.15 ± 0.05	0.06 ± 0.03	219, 26	1.16 ± 0.08	SARG	yes
HD88133	5516 ± 46	4.06 ± 0.07	1.05 ± 0.06	0.40 ± 0.04	139, 17	1.18 ± 0.09	UVES	yes
HD89307	5992 ± 17	4.49 ± 0.03	1.06 ± 0.03	-0.09 ± 0.01	240, 30	1.00 ± 0.07	ESPADONS	yes
HD89307	5961 ± 18	4.46 ± 0.03	1.00 ± 0.03	-0.12 ± 0.01	243, 31	0.98 ± 0.07	SOPHIE	no
HD89744	6381 ± 43	4.27 ± 0.05	1.70 ± 0.05	0.30 ± 0.03	145, 21	1.37 ± 0.09	SARG	yes
muAra	5784 ± 21	4.22 ± 0.04	1.07 ± 0.03	0.30 ± 0.02	242, 32	1.15 ± 0.08	HARPS	yes
muAra	5799 ± 24	4.29 ± 0.04	1.06 ± 0.03	0.31 ± 0.02	200, 24	1.13 ± 0.08	UVES	no
OGLE-TR-10	6172 ± 73	4.58 ± 0.07	1.53 ± 0.10	0.37 ± 0.06	183, 23	1.19 ± 0.08	UVES	yes
OGLE-TR-132	6180 ± 43	4.35 ± 0.05	1.41 ± 0.05	0.30 ± 0.03	177, 18	1.25 ± 0.09	UVES	yes
OGLE-TR-56	6154 ± 62	4.25 ± 0.10	1.47 ± 0.07	0.28 ± 0.05	196, 25	1.30 ± 0.10	UVES	yes
tauBoo	6617 ± 80	4.54 ± 0.10	1.82 ± 0.10	0.40 ± 0.06	141, 19	1.38 ± 0.10	ESPADONS	no
tauBoo	6659 ± 84	4.57 ± 0.10	1.94 ± 0.10	0.40 ± 0.06	140, 21	1.38 ± 0.10	UVES	yes
TrES-1	5285 ± 45	4.37 ± 0.09	0.96 ± 0.08	0.08 ± 0.03	188, 24	0.87 ± 0.07	UVES	yes